Mapping potential cyanobacterial bloom using Hyperion/EO-1 data in Patos Lagoon estuary

Mapeamento de potenciais florações de cianobactérias usando imagem Hyperion/EO-1 no estuário da Lagoa dos Patos

Lobo, FL.[1], Barbosa, CC.[1], Novo, EMML.[1] and Yunes, JS.[2]

[1]Divisão de Sensoriamento Remoto – DSR, Instituto Nacional de Pesquisas Espaciais – INPE,
CP 515, CEP 12201-970, São José dos Campos, SP, Brazil
e-mail: lobo@dsr.inpe.br; claudio@dpi.inpe.br; evlyn@dsr.inpe.br

[2]Unidade de Pesquisa em Cianobactérias – UPC, Universidade Federal do Rio Grande – UFRG,
CP 474, CEP 96201-900, Rio Grande, RS, Brazil
e-mail: jsyunes@furg.br

Abstract: Aim: This paper proposes an approach for using remote sensing data for identification and mapping of cyanobacterial blooms; **Methods:** It uses two sets of spectra (empirical and theoretical) as reference to classify the areas of cyanobacteria blooms using a Hyperion image acquired over the Patos Lagoon, located in Rio Grande do Sul State, Brazil. To circumvent cyanobacteria misclassification due to suspended inorganic particle (SIP) scattering, pigment band ratios – phycocyanin (650/620 nm) and chlorophyll-*a* (700/680 nm) - were applied; **Results:** An area of 22.5 km² prone to cyanobacterial blooms was mapped into 5 classes with chlorophyll-*a* concentration varying from 8 to 1,000 µg.L^{-1} using both, empirical and theoretical spectra; **Conclusions:** The results corroborate the general spectral features of cyanobacterial blooms and indicated that band ratios operation removed the areas affected by high concentrations of SIP.

Keywords: phycocyanin, chlorophyll-*a*, remote sensing, hyperespectral, Patos Lagoon.

Resumo: Objetivo: Este artigo apresenta um método de identificação e mapeamento de florações de cianobatérias utilizando imagem do sensor hiperespectral Hyperion/EO-1; **Métodos:** O método aplica dois conjuntos de curvas espectrais (uma empírica e outra teórica) como referência para classificar áreas potenciais de ocorrência de cianobactérias na Lagoa dos Patos localizada no Estado do Rio Grande do Sul Rio Grande, Brasil. De modo a evitar que partículas inorgânicas fossem indevidamente classificadas como cianobactérias devido ao espalhamento da radiação por partículas inorgânicas em suspensão (PIS) foi realizada a intersecção das áreas resultantes do cálculo da razão entre as bandas referentes às absorções pela ficocianina (650/620 nm) e clorofila-a (700/680 nm); **Resultados:** Uma área total de 22,5 km² potencial na ocorrência de cianobactéria foi identificada e classificada em 5 classes de concentrações de clorofila-a variando entre 8 e 1000 µg.L^{-1} a partir dos conjuntos de espectros de referência – empírico e teórico – com 88% de similaridade entre eles; **Conclusões:** Os resultados corroboram as feições espectrais de florações de cianobactérias e indicam que as áreas afetadas pelo efeito de espalhamento pela presença de altas concentrações de PIS foram removidas pela metodologia aplicada.

Palavras-chave: ficocianina, clorofila-*a*, sensoriamento remoto, hiperespectral, Lagoa dos Patos.

1. Introduction

Algal blooms represent a significant and growing threat to aquatic systems, since it spoils the water quality for human and ecological uses. Some algae genera produce toxins, which can be harmful to human healthy and fisheries. The occurrence of cyanobacterial blooms, mainly the genera *Aphanothece* sp., *Anabaena* sp. and *Microcystis* sp. in the Patos Lagoon located in Rio Grande do Sul state, has been reported since early 1980's (Betito, 1984; Matthiensen et al., 1999; Yunes, 2009). Those authors relate the blooms to the increasing water pollution from untreated domestic and industrial sewage from Rio Grande urban area. The sewage increases the nutrient input beyond natural level

and triggers the environmental set for bloom outbreak at Arraial and Mangueira bays.

Ever since, the frequency and density of blooms increased up to a level that Mangueira bay was included in the list of world's dead zones (Diaz and Rosenberg, 2008) due to the constant extremely low Dissolved Oxygen concentration (DO) and high eutrophication levels. Those two variables are detrimental to aquatic system biodiversity because they favor algae groups with wider environmental requirements such as cyanobacteria. This group can intake atmosphere oxygen, and control light availability by moving up and down in the water column, affecting the entire

trophic chain and water resources availability for life support (Yunes et al., 1996; Metsamaa, 2005).

In spite of being well known the cyanobacteria genera and the factors controlling the blooms in Patos Lagoon, there is a lack of information of its spatial distribution due to the large area of the estuary (900 km²), which prevents the use of classical water sampling techniques due to time and cost constraints.

Remote sensing techniques, however, can be used to detect optical properties of cyanobacteria population (Brando and Dekker, 2003; Kutser et al., 2001; Han and Rundquist, 1997) contributing to improve spatial and temporal information on bloom distribution. The launch of the Hyperion Imaging Spectrometer, the first high spatial resolution imaging spectrometer to successfully orbit the Earth, increased the potential of not only detecting algae blooms, but also, distinguishing cyanobacteria out of them (Brando and Dekker, 2003).

The use of remote sensing images to study the distribution of algae blooms is based on the fact that algae pigments affect the color of the water body (Folkestad et al., 2007). Algae photo-synthesizer pigments are optically active components (OAC) and absorb electromagnetic radiation in specific wavebands (Kirk, 1994). However, there are other optically active components such as dissolved organic matter (DOM) and suspended inorganic particles (SIP), which also can interact with the incoming radiation and, sometimes, decrease the accuracy of the optical determination of the algae dominant pigment (Mobley, 1994). That has prevented the operational use of multi-spectral sensors for inland and coastal water monitoring in the past (Galvão et al., 2003).

Cyanobacteria is characterized by accessory pigments (phycobiliproteins) which favors the absorption of electromagnetic radiation in wavelengths other than that of chlorophyll-*a* taking advantage of a wider range of the available photosynthetic radiation (Kirk, 1994; Wynne et al., 2008).

The three main pigment groups controlling cyanobacteria optical properties are: chlorophyll-*a*, with absorption bands in 440 and 675 nm; carotene, with absorption at ultra-violet and blue region; and phycobiliproteins, which are exclusive of cyanobacteria, with absorption band at 620 nm and fluorescence band at 650 nm (Johnsen et al., 1994).

It is also typical a maximum of phytoplankton scattering in green wavelengths produced by difference in refractive index of water and cell walls (Gitelson, 1992). This maximum, however, can shift towards longer wavelengths with the increasing chlorophyll-*a* concentration and cell density (Londe, 2008).

The phycobiliprotein absorption band (620 nm), phycocyanin in freshwater systems, is therefore a marker for cyanobacteria presence in eutrophic inland water (Kutser,

2004). Hyperspectral sensors circumvent the limitations of multispectral remote sensing application to operational eutrophication (Han, 2005), because they provide for narrow bands (<10 nm) which can pick up more specific absorption bands.

There are two approaches currently in use for deriving the concentration of OAC from hyperspectral images. The first is based on semi-analytical models through which the inherent optical properties (IOP) are derived, that is to say their scattering and absorption coefficients. Those coefficients are input to models, which uncouple the pigment concentration (Chl-*a*), suspended inorganic particle concentration (SIP) and dissolved organic matter concentration (DOM). Those approaches are fully described Giardino et al. (2007) and Mestamaa (2005).

The second approach to derive OAC concentration is based on empirical models. These models relate water surface reflectance (R%) at several spectral bands to in situ measurements of OAC concentration. They are well described in Lee et al. (1995), Simis et al. (2005) and Yang and Pan (2006).

This paper proposes an alternative approach for using remote sensing data for identification and mapping of cyanobacterial blooms in Patos Lagoon estuary. The method is based upon two sets of reference spectra (theoretical and empirical) to emphasize their similarity disregarding the way they were produced. The classifier compares the spectra of each Hyperion image pixel acquired over Patos Lagoon to the reference spectra representing different water types regarding pigment concentration, allowing for the identification of potential areas of cyanobacterial blooms.

2. Material and Methods

2.1. Study area

Patos Lagoon is the largest lagoonal complex in South America and connects to the South Atlantic via a 20 km entrance channel 0.5-3 km in width (Figure 1). Physicochemical dynamics of Patos Lagoon estuary are determined by topographical and meteorological conditions, with the tidal range within the estuary limited to low diurnal amplitude (mean = 0.47 m). The main nutrient load in the estuary derives from land runoff of the drainage basin, domestic and industrial sewage from adjacent cities (Rio Grande and Pelotas, approximately 500,000 inhabitants) and the introduction of agricultural fertilizers.

2.2. Cyanobacteria spectral features and mapping strategy

The first step of this research consisted of reviewing in the literature existing spectra of algal blooms acquired under different approaches and environmental conditions and to seek for common features related to the presence of cyanobacteria disregarding the acquisition setting in laboratory under controlled conditions or in situ. Figure 2
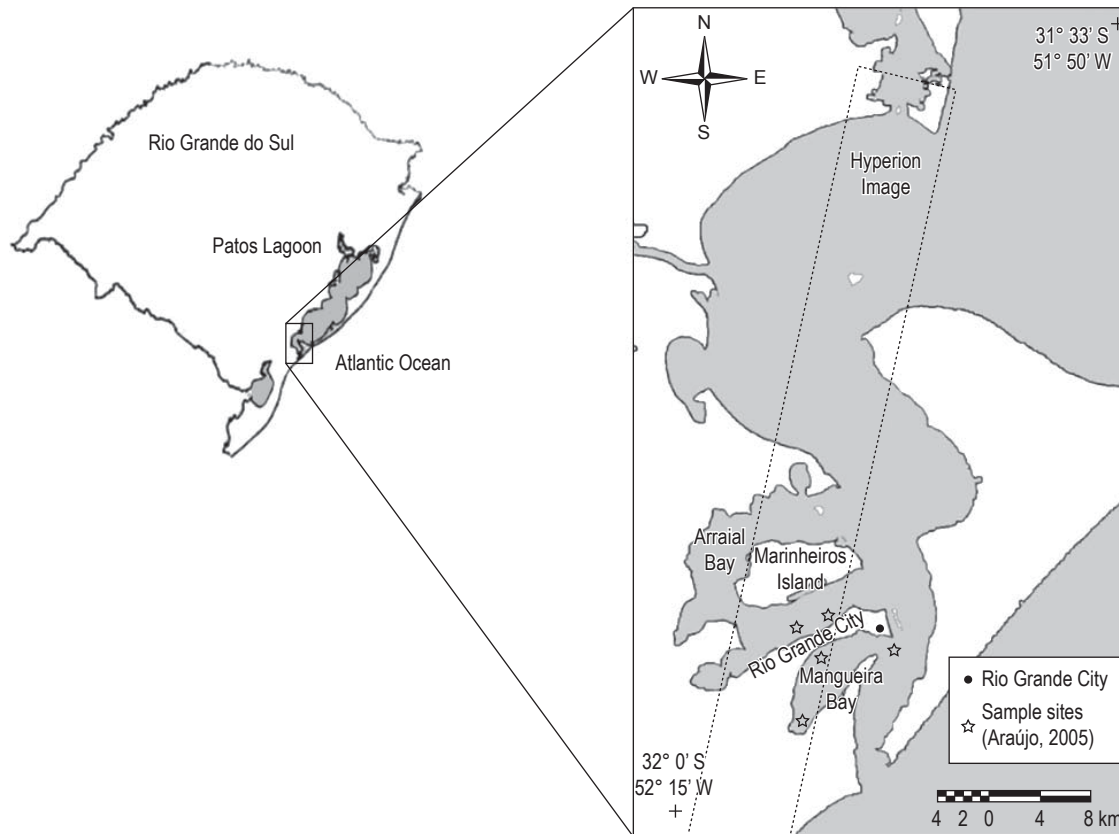
Figure 1. Patos Lagoon estuary in Rio Grande do Sul State. In the figure it is highlighted the location of the Rio Grande city ,the sampling sites of Araújo (2005) and Hyperion image.
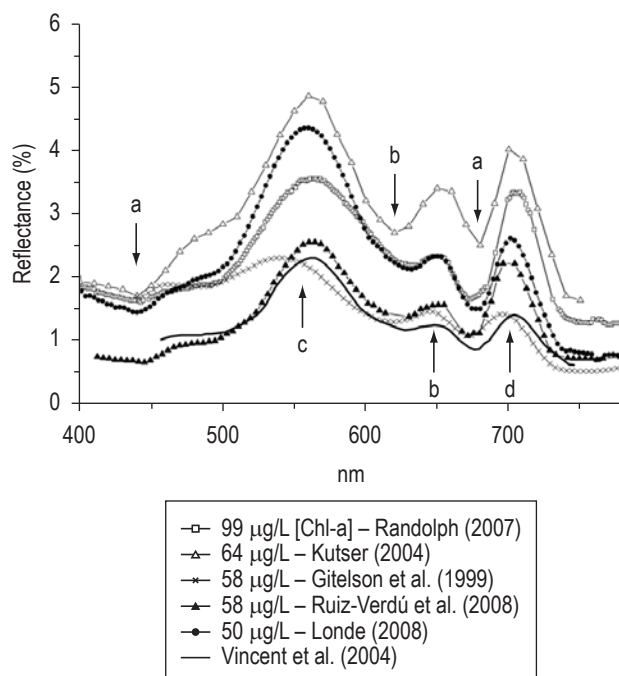

Figure 2. Spectral curves obtained at different regions and with several methods presented common cyanobacteria features: a) Chl-*a* absorption at 440 and 675 nm; b) phycocyanin absorption at 620 nm and fluorescence at 650 nm; c) scattering in the green region; d) near-infrared scattering by phytoplankton cells.

summarizes the general spectral features characterizing cyanobacteria at several Chl-*a* concentrations based on literature results (Gitelson et al., 1999; Kutser, 2004; Vincent et al., 2004; Randolph et al., 2007; Londe, 2008; Ruiz-Verdú et al., 2008).

The main features common to all spectra, disregarding the chlorophyll concentration are the absorption band at 620 nm and the fluorescence band at 650 nm, which become more outstanding as Chl-*a* concentration increases. Other features common to other algae genera are the absorption band in the blue, the maximum scattering in the green and in the near infrared (NIR).

In the second phase of this study is presented the strategy used for identifying and mapping the potential areas of cyanobacteria based on Hyperion images (Figure 3).

2.3. Hyperion/EO-1 image classification

The sensor Hyperion, on board of the satellite Earth Observing One (EO-1), provides 7.5 by 100 km scenes with 220 spectral bands fit in the spectral range between 400 and 2500 nm and 30 × 30 m spatial resolution. The Hyperion scene used in this study was acquired in May/07, 2003 (Figure 1) which was atmospherically corrected using a radiative transfer model implemented in the FLAASH algorithm available in the software ENVI 4.4.
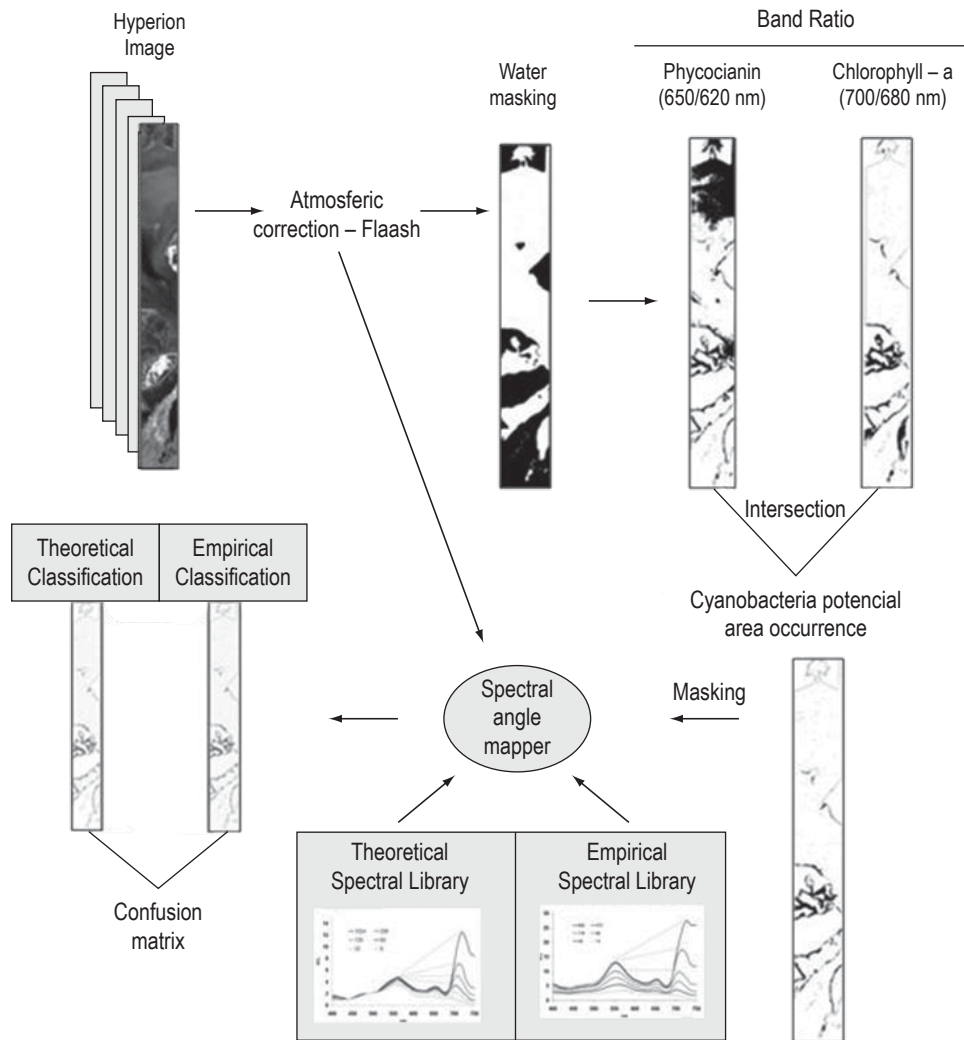
Figure 3. Steps followed to identify and map cyanobacteria bloom using Hyperion images.

The next step was to build a water mask using the near-infrared bands (850-900 nm) in which there are the largest contrast between water reflectance and typical land cover (Rudorff, 2007). This procedure reduces the computation time and increases classification accuracy by removing land targets with similar spectral signatures.

The masked scene was used to build the ratio images using as input the PC fluorescence and absorption bands (650/620 nm) and the Chl-*a* (700/680 nm) scattering and absorption bands. The resulting images allowed identifying the potential areas of cyanobacterial blooms. A classification threshold was empirically defined by analyzing several spectra of those blooms.

The algorithm Spectral Angle Mapper (SAM) was applied to identify the potential areas of cyanobacterial blooms. SAM determines the spectral similarity between two spectra by computing the angle between them, since it assumes that each spectrum can be described as a vector in n-dimensional space where n is the number of spectral

bands. An import feature in the SAM method is that it uses only the vector direction and not its length to calculate the spectral angle between an input and a reference spectrum. That means that the method is not sensitive to spectra intensity changes. The spectral intensity may change due to both changes in IOP concentration or because of residual atmospheric effects. Assuming that the IOP remains constant for a given pixel, atmospheric and other environmental effects can be neglected. However, as generally common to all supervised algorithms, SAM accuracy is highly sensitive to the choice of reference spectra (Barbosa, 2005). Therefore, the most critical step was to define and validate sets of reference spectra for quantifying Chl-*a* concentration, since in the majority of available spectra that is the only measured pigment.

2.4. Empirical and theoretical reference spectra

The first set of reference spectra was based on 36 samples acquired at Ibitinga Reservoir, São Paulo State (Londe,

2008). Downwelling radiance and upwelling total radiance measurements were collected at each of the sampling sites using an ASD FieldSpec UV–VNIR (Analytical Devices, Inc., Boulder, CO) spectroradiometer. Radiometry was carried out simultaneously to ground sample acquisition for Chl-*a* and algae species assessment. Londe (2008) reported the dominance of *Microcystis* and *Anabaena* blooms, at Chl-*a* concentrations varying from 5 to 1,000 μg.L⁻¹, and low concentration of SIP. Those spectra were clustered into 5 classes of Chl-*a* concentration and the average Chl-*a* concentration of each class was computed. Next, the SAM algorithm was used to classify all the spectra into five classes using the average spectra as reference. That was a way of validating the empirical set of spectra and determining how far the average spectra could be representative of individual samples.

Another set of reference spectra was obtained in literature. Kutser (2004) implemented the set using a semi-analytical model. The author used Inherent Optical Properties measured previously in the Baltic Ocean to build 10 spectra with Chl-*a* concentration varying 2 to 1,024 μg.L⁻¹ as reference to map cyanobacteria blooms with Hyperion images. The model kept SIP and dissolved organic matter (DOM) concentration low and constant varying only the Chl-*a* concentration.

2.5. Reference spectra normalization

Because the number of classes and the of Chl-*a* concentration interval varied in both theoretical and empirical spectra sets five classes of Chl-*a* concentration were defined to normalize them. The normalization was needed to allow the comparison between the classification results provided by each of the reference sets. The number of classes, five, was selected to cover the entire range of chlorophyll concentration reported in cyanobacterial blooms in the literature (Figure 4). Class A has chlorophyll-*a* concentration smaller than 32 μg.L⁻¹, Class B has Chl-*a* in the range between 33 and 70 μg.L⁻¹; class C in the range between 80 and 200 μg.L⁻¹; Class D, between 250 e 600 μg.L⁻¹; and Class E Chl-*a* larger than 700 μg.L⁻¹.

2.6. Classification and confusion matrix analyses

Once the five classes were defined they were used as empirical and theoretical libraries to run the SAM algorithm in the spectral range between 450 and 750 nm. The wavebands smaller than 450 nm e larger than 750 nm were discarded because of the reported low Signal-to-Noise Ratio (SNR) of this Hyperion sensor bands. The maximum classification threshold was set 0.5 rad (Kutser, 2004), a relaxed threshold when compared to the 0.1 rad in Lobo (2009). This threshold was selected to guarantee the classification of all the pixels in one of the defined classes.

3. Results

The images derived from the ratios of phycocyanin and chlorophyll discriminating bands are presented in Figure 5.

1) Class A – 14 μg.L⁻¹ CHL-*a*; 2) Class B – 49; 3) Class C – 99; 4) Class C – 176; 5) Class D – 472; 6) Class E - 900.

1) Class A – 8 μg.L⁻¹ CHL-*a*; 2) Class B - 32; 3) Class B – 64; 4) Class C – 128; 5) Class D – 256; 6) Class E – 1024
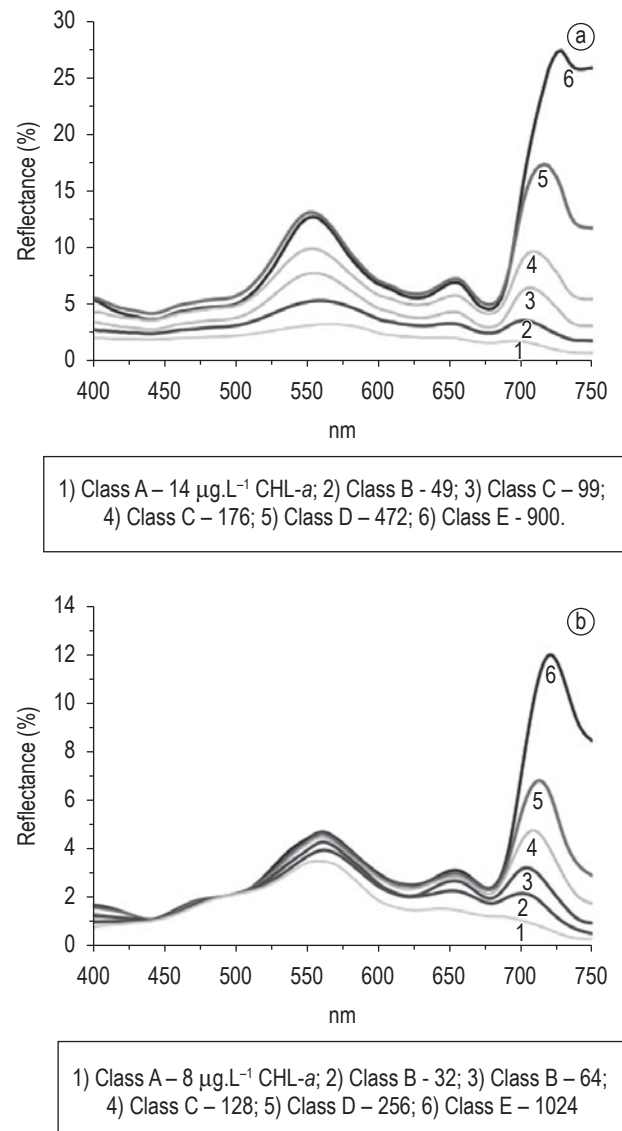
Figure 4. a) Sets of reference spectra, empirical and b) theoretical, used to classify potential cyanobaterial bloom using Hyperion images. The increased reflectance in NIR as a function of Chl-*a* concentration is highlighted in both sets.

Figure 5a is the phycocyanin ratio (R_{PC}) between 650 nm (phycocianin fluorescence maximum) and 620 nm (phycocyanin absorption band), which enhances cyanobacterial blooms. Figure 5b is the chlorophyll ratio ($R_{Chl}a$) between 700 nm (algae cell scattering) and 680 nm (Chl-*a* absorption band), which enhances the presence of chlorophyll distribution. The R_{PC} image includes an area larger than that of the R_{Chl-a}, 105 e 35 km² respectively. Figure 5c represents the intersection of the previous distribution.

In Figure 5a, the highlighted spot show that the R_{PC} threshold of 1 includes areas of high SIP concentration (Figure 5d) responsible for a steady increase in the spectral reflectance from the red towards the near infrared (Brando and Dekker, 2003) and responds for an overestimation of cyanobacterial blooms. Figure 5b shows that in the $R_{Chl}a$
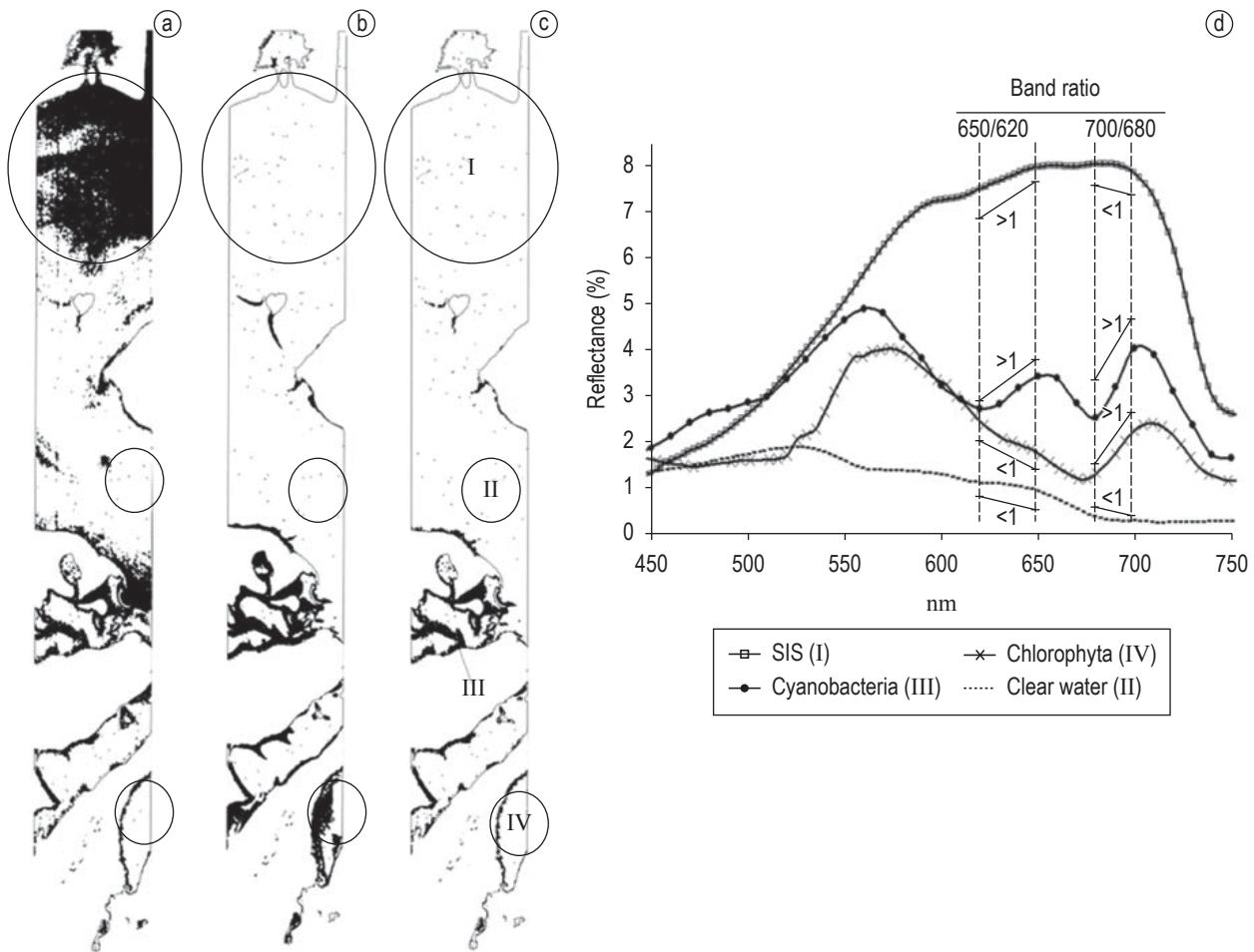
Figure 5. a) R_{PC} b) $R_{Chl\text{-}a}$ c) intersection of R_{PC} and $R_{Chl\text{-}a}$ images. In (d) the spectral reflectance of areas highlighted in I) SIS dominated water misclassified as cyanobacterial bloom; II) clear water; III) dominance of cyanobacterial bloom; IV) dominance of any other algae group bloom.

image the error related to SIP is removed (see Figure 5d), and only the areas covered by algae are classified. The image resulting from the intersection of image 5a and b displays areas with high potential of cyanobacterial blooms and were used as input for classification of their abundance.

As shown in Figure 6a and 6b, Hyperion image classification using both reference spectra sets produce results with 88% of similarity between them. The differences in classification can be observed in Table 1. The empirical reference spectra (ERS) attributed a larger number of pixels to classes A, D and E than the theoretical reference spectra (TRS). Class C presented the largest agreement (97%) in the classification results for both reference sets, followed by class B (82%), class D (86%), class A (46%) and class E (18%).

The spectra extracted from the Hyperion images for each class (Figure 7) are similar to both TRS and ERS sets (Figure 4) and, also, the maximum scattering shifted towards the longer wavebands reaching the same position as both sets of reference spectra (Table 2). The green reflec-

tance maximum, however, was kept constant at 589 nm, whereas the reference spectra maximum moved around 560 nm.

Figure 8 shows the ratio of Hyperion spectra, randomly collected, and the ERS and TRS sets normalized at 447 nm. It is clear that the Hyperion reflectance is higher than those of the reference sets, mainly in the spectral region sensitive to high SIP concentration. This difference is even larger in Class A due to the low chlorophyll-*a* concentration that can be easily masked by SIP scattering. In the classes with larger phytoplankton biomass, the pigment spectral features are more prominent (Classes D and E) and the difference between the class spectra and the reference spectra is smaller. Figure 8 also highlights that the empirical curves are more variable than the theoretical, because the concentration of other OAC was low but not constant (Londe, 2008).

4. Discussion

The difference between the potential areas of cyanobacterial blooms identified by the ratios R_{PC} and $R_{Chl\text{-}a}$ is caused

by the presence of high concentration of SIP that increases the red and NIR reflectance (Han and Rundquist, 1997). The ratio of band 650 and 620 nm is larger than 1 in those areas making it difficult to distinguish them from that of cyanobacteria (Figure 5d). On the other hand, the Chl-*a*

ratio allowed mapping different algae groups and even submerged macrophytes common in this region. According to Marangoni and Costa (2006) there were around 70 km² of macrophytes marshes in that area mixed with cyanobacterial blooms. Those marshes favor the development of cyanobacteria by reducing water velocity and increasing sedimentation that in turn increases the euphotic zone depth and nutrient storage. Moreover in the 2002/2003 summer southern Brazil was influenced by El Niño (Colling and Bemvenuti, 2007) characterized by high precipitation, which decreases water salinity and again favours the increase cyanobacteria outbreak in the region (Yunes et al., 1996). Those environmental features are recurrent in the Arraial and Mangueira bays with shallow waters (average depth of 70 cm), low turbulence, low salinity and high input of nutrients from Rio Grande City sewage.

During the entire year of 2004, Araújo (2005) monitored phytoplankton abundance in the region and confirmed the existence of *Aphanothece* and *Microcystis* in all 5 sampling sites shown in Figure 1. Both *Aphanothece* and *Microcystis* are buoyant and occur concentrated at
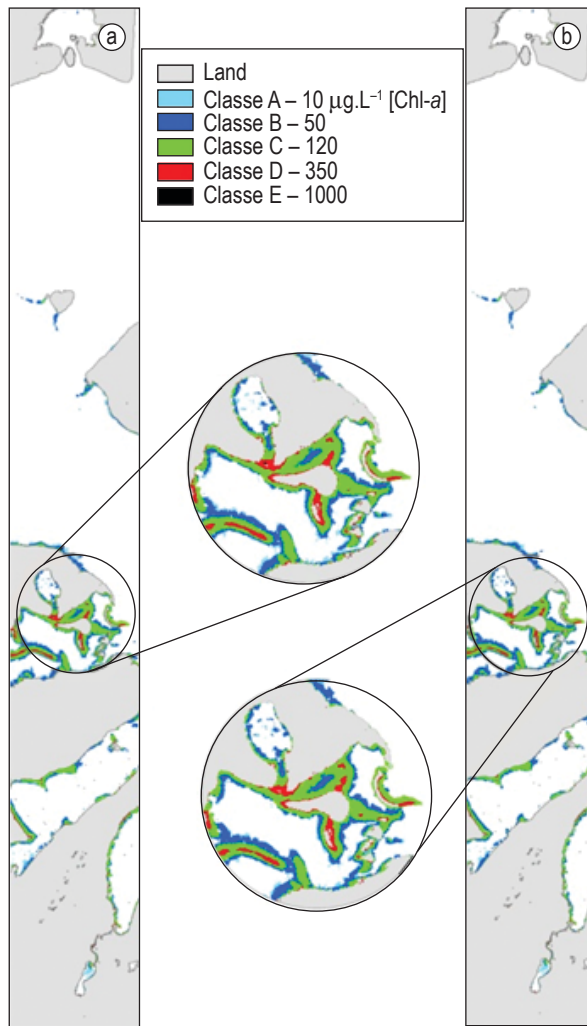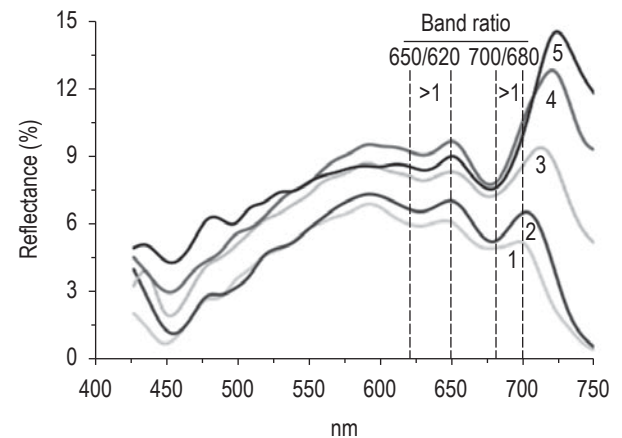

Figure 6. Cyanobacterial bloom abundance classes expressed by the chlorophyll-*a* concentration based on reference spectra empirical (a) and theoretical (b) with 88% of similarity between them.

1) Class A – 10 μg.L⁻¹ Chl-*a*   2) Class B – 50
3) Class C – 120   4) Class D – 350   5) Class E – 1000

Figure 7. Spectra randomly extracted from the Hyperion images for each class.

Table 1. Confusion matrix (in pixel) of classification results using empirical (columns) and theoretical (lines) reference spectra as input to SAM classifier.

pixel		Empirical Reference Spectra					Total
		A	B	C	D	E	
Theoretical reference spectra	A	1280	16	0	0	0	1296
	B	1530	8592	450	0	0	10572
	C	0	119	9658	683	0	10460
	D	0	0	85	2334	175	2594
	E	0	0	0	0	39	39
	Total	2810	8727	10193	3017	214	24961

Table 2. Reflectance maxima in the green (500 to 599 nm) and NIR (695 to 750 nm) for each class: empirical, theoretical and Hyperion image spectra.

Class	Empirical		Theoretical		Hyperion image	
	green	NIR	green	NIR	green	NIR
A	563	695		700		700
B	560	701		700		700
C	554	710	560	710	589	710
D	554	720		720		720
E	554	728		720		-

1) Class A   2) Class B   3) Class C
4) Class D   5) Class E

1) Class A   2) Class B   3) Class C
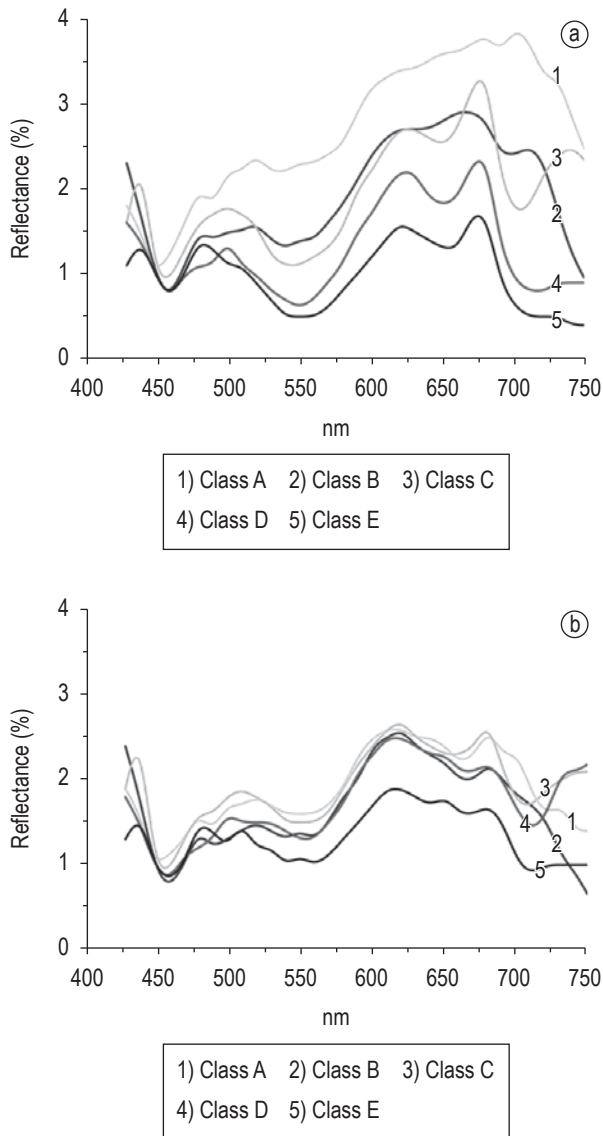4) Class D   5) Class E

Figure 8. Ratio of the Hyperion Spectra and ERS (a) and TRS (b).

the water surface what makes it easier their identification by remote sensors. Chlorophyll concentration in the *Aphanothece* group varied from 100 to 3800 μg.L⁻¹ in the Mangueira bay between May and November. In the Rio

Grande inlet Araújo (2005) identified *Microcystis botrhis* blooms at concentrations up to 4,000 μg.L⁻¹ Chl-a. The main natural forcing functions controlling the persistence and fading of algae and cyanobacteria in the Patos Lagoon estuary are related to high nutrient level and low salinity (Spengler et al., 2007) as well as northeast winds which during autumn steadily pulls phytoplankton population into the bays (Yunes et al., 1998; Becker et al., 2004; Araújo, 2005). Therefore, in spite of the lack of ground truth data concurrently to Hyperion image acquisition, the data available for the region support the results obtained with the Hyperion image of the Patos Lagoon.

The analyses of Hyperion spectra allowed identifying the absorption features of phycocyanin and chlorophyll–a pigment similar to the reference spectra sets. The three sets of spectra – empirical, theoretical and Hyperion - present the green and NIR maxima similar for Chl-a concentration between 100 and 150 μg.L⁻¹ (class C). Hyperion spectra, however, have a much higher reflectance beyond 550 nm due to the SIP effect moving the maximum of green reflectance towards higher wavelength as the particle concentration increases. In the Hyperion images the maximum of the green is reached at 589 nm, a 35 nm difference in relation to the maxima observed in the reference spectra. The difference between Hyperion spectra and both sets of reference spectra can be explained by several acquisition factors. First, Hyperion sensor integrates the energy over an area of 30 × 30 m, including a large variability in the upwelling radiation due to environmental effects such as wind, bottom depth and composition, and water volume multiple scattering over a larger area (Mobley, 1994). Than, lagoon is shallow (average of 70 cm) with uneven bottom covered mainly by fine sand (highly reflexive) and apt to add a significant signal to the upwelling radiation (Calliari et al., 2008). In spite of those differences, they present the diagnosis features, which enabled the use of hyperspectral images to map potential areas of cyanobacterial blooms.

The method proposed in this research allowed to map an area of 22.5 km² prone to cyanobacterial blooms in the Patos Lagoon estuary applying a Hyperion image acquired in May 7, 2003. The mapped areas are the Mangueira and Arraial bays which have the ideal features to support the development of cyanobacteria such as: high nutrient concentration (domestic and industrial from Rio Grande Municipality), low salinity, shallow water, low turbulence, northeast wind that traps the water within the bay.

The five classes of Chl-a concentration from 10 to 1,000 μg.L⁻¹ of cyanobacterial blooms presented similar classification results disregarding the reference spectra sets used as input to the SAM algorithm. Those sets, therefore, proved to be representative of the proposed classes and can be used in areas different than those of the image. They

can be used as reference to classify other Hyperion images acquired in the Patos Lagoon in the near future.

The results also indicate that the intersection between the R_{PC} and R_{Chl-a} removed the areas affected by high concentrations of SIP (Figure 5) but the effect of smaller SIP concentrations remains mixed to that of other optical active components.

Acknowledgements

References

ARAÚJO, EAC. *Environmental agents for cyanobacteria occurrence around Rio Grande city.* Rio Grande: Universidade Federal do Rio Grande, 2005. 120 p. [Dissertação de Mestrado].

BARBOSA, CCF. *Remote sensing of water circulation dynamic to the Curuai floodplain/Amazon river.* São José dos Campos: Instituto Nacional de Pesquisas Espaciais, 2005. p. 281. [Tese de Doutorado].

BECKER, V., CARDOSO, LS. and MARQUES, DM. Development of *Anabaena* Bory ex Bornet and Flahault (Cyanobacteria) blooms in a shallow, subtropical lake in southern Brazil. *Acta Limnol. Bras.* 2004, vol. 16, no. 4, p. 306-317.

BETITO, R. *Population dynamics of Jenyasis lineatana in Patos Lagoon salt marsh.* Rio Grande: Universidade Federal do Rio Grande, 1984. 207 p. [Dissertação de Mestrado].

BRANDO, VE. and DEKKER, AG. Satellite hyperspectral remote sensing for estimating estuarine and coastal water quality. *IEEE Trans. Geosci. Remote Sens.* 2003, vol. 41, no. 6, p. 1378-1387.

CALLIARI, LJ., WINTERWERP, JC., FERNANDESA, E., CUCHIARAA, D., VINZOND, SB., SPERLE, M. and HOLLAND, KT. Fine grain sediment transport and deposition in the Patos Lagoon-Cassino beach sedimentary system. *Cont. Shelf Res.* 2008. (no prelo).

COLLING, LA. and BEMVENUTI, CE. The El Niño 2002/2003 in Patos Lagoon estuary: influences in macrozoobenthos, RS, Brazil. In *Anais do VIII Congresso de Ecologia do Brasil*, Setembro 23-28, 2007. Caxambú, 2007.

DIAZ, RJ. and ROSENBERG, R. Dead zones and consequences for marine ecosystems. *Science.* 2008, vol. 321, no. 5891, p. 926-929.

FOLKESTAD, A., PETTERSSON, LH. and DURAND, DD. Inter-comparison of ocean colour data products during algal blooms in the Skagerrak. *Int. J. Remote Sens.* 2007, vol. 28, no. 3, p. 569-592.

GALVÃO, LS., PERREIRA-FILHO, W., ABDON, MM., NOVO, EMML., SILVA, JSV. and PONZONI, FJ. Spectral reflectance characterization of shallow lakes from the Brazilian Pantanal wetlands with field and airborne hyperspectral data. *Int. J. Remote Sens.* 2003, vol. 24, no. 21, p. 4093-4112.

GIARDINO, C., BRANDO, V., DEKKER, AG., STROMBECK, N. and CANDIANI, G. Assessment of water quality in Lake Garda (Italy) using Hyperion. *Remote Sens. Environ.* 2007, vol. 109, no. 2, p. 183-195.

GITELSON, AA. The peak near 700 nm on radiance spectra of algae and water: relationships of its magnitude and position with chlorophyll concentration. *Int. J. Remote Sens.* 1992, vol. 13, no. 17, p. 3367-3373.

GITELSON, AA., SCHALLES, JF., RUNDQUIST, DC., SCHIEBE, FR. and YACOBI, YZ. Comparative reflectance properties of algal cultures with manipulated densities. *J. Appl. Phyc.* 1999, vol. 11, no. 4, p. 345-354.

HAN, L. and RUNDQUIST, DC. Comparison of NIR/RED ratio and first derivative reflectance in estimating algal-chlorophyll concentration: a case study in a turbid reservoir. *Remote Sens. Environ.* 1997, vol. 62, no. 3, p. 253-261.

HAN, L. Estimating chlorophyll-a concentration using first-derivative spectra in coastal water. *Int. J. Remote Sens.* 2005, vol. 26, no. 23, p. 5235-5244.

JOHNSEN, G., SAMSET, O., GRANSKOG, L. and SAKSHAUG, E. In vivo absorption characteristics in 10 classes of bloom-forming phytoplankton: taxonomic. *Mar. Ecol. Prog. Ser.* 1994, vol. 105, no. 1, p. 149-157.

KIRK, JTO. *Light and photosynthesis in aquatic systems.* Cambridge: Cambridge University Press, 1994. p. 528.

KUTSER, T. Quantitative detection of chlorophyll in cyanobacterial blooms by satellite remote sensing. *Limnol. Oceanogr.* 2004, vol. 49, no. 6, p. 2179-2189.

KUTSER, T., HERLEVI, A., KALLIO, K. and ARST, H. A hyperspectral model for interpretation of passive optical remote sensing data from turbid lakes. *Sci. Total Environ.* 2001, vol. 268, no. 1-3, p. 47-58.

LOBO, FL. *Biblioteca espectral*: determinação de espectros de referência para classes de tipos de água das áreas alagáveis da Amazônia. São José dos Campos: Instituto Nacional de Pesquisas Espaciais, 2009. 132 p. [Dissertação de Mestrado].

LONDE, LR. *Phytoplankton spectral behavior of a Brazilian eutrophic reservoir, Ibitinga, SP*. São José dos Campos: Instituto Nacional de Pesquisas Espaciais, 2008. 200 p. [Tese de Doutorado].

LEE, TY., TSUZUKI, M., TAKEUCHI, T., YOKOYAMA, K. and KARUBE, I. Quantitative determination of cyanobacteria in mixed phytoplankton assemblages by an in vivo fluorimetric method. *Anal. Chim. Acta.* 1995, vol. 302, no. 1, p. 81-87.

MARANGONI, JC. and COSTA, CSB. Temporal variability of marismas distribution in Patos Lagoon estuary: anthropogenic pressure and natural processes. In *Abstract of I Ocean and Coastal Ecosystems Symposium*, 2006. Salvador, 2006.

MATTHIENSEN, A., YUNES, JS. and COOD, GA. Occurrence, distribution and toxicity of cyanobacteria from the Patos Lagoon estuary, Southern Brazil. *Rev. Bras. Biol.* 1999, vol. 59, no. 3, p. 1-15.

MESTAMAA, L. *Detecting cyanobacterial blooms by passive optical remote sensing-the Baltic Sea*: case study. Tartu: University of Tartu, 2005. 94 p. [Dissertação de Mestrado].

MOBLEY, CD. *Light and water*: radiative transfer in natural waters. San Diego: Academic, 1994. 592 p.

RANDOLPH, KL. *Remote sensing of cyanobacteria in case II waters using optically active pigments, chlorophyll a and phycocyanin*. Indiana: Indiana University, 2007. 144 p. [Dissertação de Mestrado].

RUDORFF, CM., NOVO, ELM., GALVÃO, LS. and PEREIRA-FILHO, W. Derivative analysis of hyperspectral data measured at field and orbital level to characterize the composition of optically complex waters in Amazon. *Acta Amazon.* 2007, vol. 37, no. 2, p. 269-280.

RUIZ-VERDÚ, A., SIMIS, SGH., HOYOS, D., GONS, HJ. and PEÑA-MARTÍNEZ, R. An evaluation of algorithms for the remote sensing of cyanobacterial biomass. *Remote Sens. Environ.* 2008. (no prelo).

SPENGLER, A., WALLNER-KERSANACH, M. and BAUMGARTEN, MGZ. Rio Grande municipal dump site impact in the estuary of the Patos Lagoon (RS, Brazil). *Acta Limno. Bras.* 2007, vol. 19, no. 2, p.197-210.

SIMIS, SGH., PETERS, SWM. and GONS, HJ. Remote sensing of the cyanobacterial pigment phycocyanin in turbid inland water. *Limnol. Oceanogr.* 2005, vol. 50, no. 1, p. 237-245.

VINCENT, RK., QIN, X., MCKAY, ML., MINER, J., CZAJKOWSKI, K., SAVINO, J. and BRIDGEMAN, T. Phycocyanin detection from LANDSAT TM data for mapping cyanobacterial blooms in Lake Erie. *Remote Sens. Environ.* 2004, vol. 89, no. 4, p. 381-392.

WYNNE, TT., STUMPF, RP., TOMLINSON, MC., WARNER, RA., TESTER, PA., DYBLE, J. and FAHNENSTIEL, GL. Relating spectral shape to cyanobacterial blooms in the Laurentian Great Lakes. *Int. J. Remote Sens.* 2008, vol. 29, no. 12, p. 3665-3672.

YANG, D. and PAN D. Hyperspectral retrieval model of phycocyanin in case II waters. Chinese *Sci. Bull.* 2006, vol. 51, no. 2, p. 149-153.

YUNES, JS., SALOMON, A., MATTHIENSEN, A., COOD, GA. and BEATTIE, KA. Toxic blooms of cyanobacteria in the Patos Lagoon Estuary, Southern Brazil. *Jour. Aquat. Ecossist. Health.* 1996, vol. 5, no. 4, p. 223-229.

YUNES, JS., NIENCHESKI, LFH., SALOMON, PS., PARISE, M., BEATTIE, KA., RAGGET, S. and CODD, G. Effect of nutrients balance and physical factors on blooms of toxic cyanobacteria in the Patos Lagoon, southern Brazil. *Verh. Internat. Verein. Limnol.* 1998, vol. 26, no. 1, p. 1796-1800.

YUNES, JS. Florações de *Microcystis* na Lagoa dos Patos e o seu Estuário: 20 anos de estudo. *Oecol. bras.* 2009, vol. 13, no. 2, p. 313-318.